ELSEVIER

Surface Science 486 (2001) L519–L523

SURFACE SCIENCE

www.elsevier.nl/locate/susc

Surface Science Letters

Non-dipolar contributions in XPS detection of X-ray standing waves

F. Schreiber [a,b,*], K.A. Ritley [a,b], I.A. Vartanyants [b,c,1], H. Dosch [a,b], J. Zegenhagen [d], B.C.C. Cowie [d]

[a] *Institut für Theoretische und Angewandte Physik, Universität Stuttgart, Pfaffenwaldring 57, D-70550 Stuttgart, Germany*
[b] *Max-Planck-Institut für Metallforschung, Heisenbergstrasse 1, D-70569 Stuttgart, Germany*
[c] *Institute of Crystallography RAS, Leninsky pr. 59, 117333 Moscow, Russian Federation*
[d] *ESRF, B.P. 220, F-38043 Grenoble Cedex, France*

Received 29 September 2000; accepted for publication 4 January 2001

Abstract

The analysis of X-ray standing wave (XSW) data for the determination of structural parameters of adsorbates (coherent position, P_C^h, and coherent fraction, F_C^h) is usually done in the dipole approximation. Using carbon and oxygen containing molecular adsorbates on Ag(1 1 1), we show how the non-dipolar contributions can be quantified and that they can have a strong impact on the resulting P_C^h and F_C^h. The results are particularly important for XPS detection of XSW intensities from light elements, for which fluorescence detection does not work. Moreover, we discuss how the XSW technique allows determining both the amplitude and the phase from quadrupole contributions in photoelectric scattering.

Keywords: X-ray standing waves; Surface structure, morphology, roughness, and topography; Photoelectron spectroscopy

1. Introduction

The X-ray standing wave (XSW) technique is one of the most precise tools for the determination of surface structures and adsorbate sites [1,2]. As shown schematically in Fig. 1, it exploits the yield, Y_p, of a spectroscopic signal characteristic for the adsorbate (such as XPS, Auger electrons, or X-ray fluorescence) in the XSW field caused by the coherent superposition of the incoming wave, E_0, and the Bragg-reflected wave, E_h,

$$I^{SW} = \left[1 + \left|\frac{E_h}{E_0}\right|^2 + 2C\left|\frac{E_h}{E_0}\right|\cos(v + \mathbf{hr})\right], \qquad (1)$$

where v is the phase of the complex amplitude ratio, $E_h/E_0 = |E_h/E_0|\exp(iv)$, $\mathbf{h}$ the reciprocal lattice vector multiplied by 2π, C the polarization factor ($C = 1$ for σ-polarization; $C = \cos 2\theta_B$ for π-polarization), and θ_B the Bragg angle.

XSW data are usually analyzed in the so-called dipole approximation, leading to Y_p being

* Corresponding author. Address: Max-Planck-Institut für Metallforschung, Heisenbergstrasse 1, D-70569 Stuttgart, Germany. Tel.: +49-711-689-1925; fax: +49-711-689-1902.
E-mail address: fschreib@dxray.mpi-stuttgart.mpg.de (F. Schreiber).
[1] Present address: Department of Physics, University of Illinois, 1110 W. Green Street, Urbana, IL 61801, USA.

0039-6028/01/$ - see front matter
PII: S0039-6028(01)00993-1

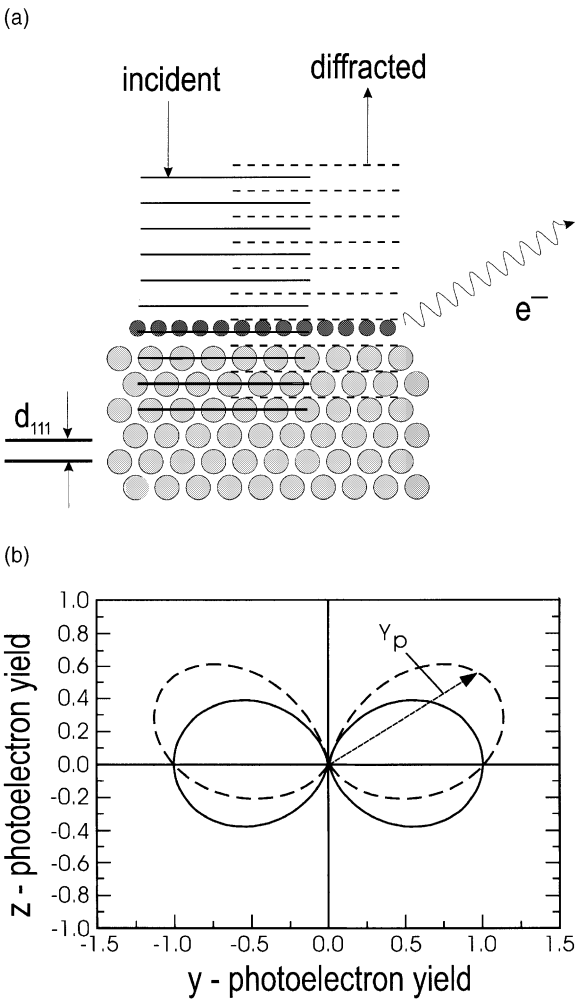

Fig. 1. (a) Schematic of the XSW technique in normal incidence geometry. In most applications, a monolayer of absorbates (dark spheres) is studied as shown. For the present study, the absorbate actually consists of several layers resulting in a film incoherent with the XSW field periodicity (not shown for clarity). (b) Schematic of the photoelectron emission cone with the length of the arrow indicating the amplitude of the yield, Y_p, in a given direction. The solid line corresponds to the pure dipolar case (symmetric about the surface at $z = 0$). The broken line schematically shows the possible asymmetry due to non-dipolar corrections.

proportional to I^{SW}. For a distribution of atoms this can be written as

$$Y_p = 1 + R + 2C\sqrt{R}F_C^h \cos(v - 2\pi P_C^h), \quad (2)$$

where $R = |E_h/E_0|^2$ is the reflectivity of the Bragg peak. The coherent position, $2\pi P_C^h = -\mathbf{hr}_C$, and the coherent fraction, $F_C^h = \langle \exp[i\mathbf{h}(\mathbf{r} - \mathbf{r}_C)] \rangle$, are the two principal parameters of the XSW technique, which are related to the average position, $\mathbf{r}_C$, of the adsorbates and the distribution around it [1,2]. In the case of a random distribution of atoms on the surface or a thick incoherent film we have $F_C^h = 0$ and, thus, simply $Y_p = 1 + R$.

However, the validity of the dipole approximation is not always obvious. Various authors have recognized the importance of multipole effects in XPS detection and the role of the angular momentum state (s, p, d, etc.) for the angular distribution of Y_p for specific experimental situations [3–7]. In contrast to the pure dipolar case, an important feature of non-dipole contributions is an asymmetry in the XPS intensity between forward and backward scattering relative to the incident beam. Recently, Vartanyants and Zegenhagen [8] developed a general formalism, which rigorously includes multipole effects, resulting in

$$Y_p = 1 + S_R R + 2|S_I|\sqrt{R}F_C^h \cos(v - 2\pi P_C^h + \psi). \quad (3)$$

The parameters S_R and $S_I = |S_I| \exp(i\psi)$ are related to the matrix elements describing the photoelectric scattering process. These include all higher-order transitions (i.e., not only dipole, but also quadrupole, octupole, etc.) [8]. S_R and S_I depend on the initial bound electron state, the photoionization energy, and the geometry of the experiment. As shown in Refs. [5,8], for the case of an initial s-state and backreflection geometry ($2\theta_B = 180°$) employed in the present experiment, one obtains

$$Y_p = \Big\{ [1 - Q'] + [1 + Q']R + 2\sqrt{R}F_C^h \mathrm{Re}\Big[(1 + iQ'') e^{i(v - 2\pi P_C^h)} \Big] \Big\}, \quad (4)$$

where $Q' = \gamma' \cos\theta_p$ and $Q'' = \gamma'' \cos\theta_p$ represent the lowest-order non-dipole (actually, cross-dipole–quadrupole) terms in photoelectric scattering. θ_p is the angle between the crystal surface normal and the position of the photoelectron detector. γ' and γ'' are defined via

$$\gamma = \gamma' + i\gamma'' = \gamma_0 \exp(i\Delta), \quad \gamma_0 = \frac{\rho_d^Q}{\rho_p^D}, \quad \Delta = \delta_d - \delta_p, \quad (5)$$

where

$$\rho_{\mathrm{p}}^{\mathrm{D}} = \int_0^\infty R_{k_{\mathrm{p}}l'=1}(r) r^3 R_{nl=0}(r)\,\mathrm{d}r,$$
$$\rho_{\mathrm{d}}^{\mathrm{Q}} = \int_0^\infty R_{k_{\mathrm{p}}l'=2}(r) r^4 R_{nl=0}(r)\,\mathrm{d}r \quad (6)$$

are dipole and quadrupole integrals ($R_{nl}(r)$ and $R_{k_{\mathrm{p}}l'}(r)$ are, respectively, the radial wave functions of the electron in the initial and final states) and δ_{p} and δ_{d} are the partial phase shifts of the final electron p- and d-state.

In the case of $F_{\mathrm{C}}^h = 0$ we obtain for the normalized yield including dipole–quadrupole cross-terms [8]

$$Y_{\mathrm{p}} = 1 + \frac{[1+Q']}{[1-Q']} R. \quad (7)$$

In this limit the photoelectron yield depends only on one non-dipole parameter, Q', which can thus be determined in a straightforward manner. For non-dipolar contributions $Q' > 0$ the yield is enhanced in comparison to the pure dipolar case ($Y_{\mathrm{p}} = 1 + R$).

2. Experimental

The experiments were performed at beamline ID32 of the European Synchrotron Radiation Facility (ESRF) in Grenoble, France. The substrate was mounted on a variable-temperature, high-precision manipulator in a UHV chamber equipped with a sputter gun for surface cleaning and a quartz crystal microbalance for thickness calibration of the adsorbate. The data reported here were taken at a sample temperature of 180 K. The backreflection condition for the Ag(1 1 1) substrate with its lattice spacing $d_{1\,1\,1}$ of 2.35 Å corresponds to an X-ray energy E_{B} around 2633 eV. A hemispherical electron analyzer (Physical Electronics) placed in the plane of the electric field vector at $\theta_{\mathrm{p}} = 45°$ away from the incoming X-ray beam was used for detection of photoelectrons and Auger electrons.

After cleaning the substrate by repeated sputter and anneal cycles, PTCDA (3,4,9,10-perylenetetracarboxylic dianhydride) was evaporated from a custom-built Knudsen cell at low flux (less than 1 ML/min). PTCDA ($C_{24}H_8O_6$), a model substance in organic molecular beam deposition [9,10], was chosen since it contains a sufficient number of carbon and oxygen atoms and since its evaporation and growth characteristics are well known. We note that the preparation conditions were not crucial, since in the present context the goal was simply to grow a film sufficiently thick to be incoherent with the substrate. This was safely accomplished for thicknesses of 10 ML (32 Å) and above, which was confirmed by thickness dependent measurements (not shown). Moreover, this can be seen from a calculation of the phase factor for N monolayers, $\varphi = |h_{1\,1\,1}|(d_{\mathrm{film}} - d_{1\,1\,1})N$, which determines F_{C}^h. With the out-of-plane lattice parameter of the film, $d_{\mathrm{film}} = 3.2$ Å, for $N = 10$ one obtains $\varphi = 22.7 \sim 7\pi$, i.e., the phase changes strongly across the film, so that it is effectively incoherent with the substrate.

While scanning the photon energy through the Bragg condition, C(1s) and O(1s) XPS as well as oxygen Auger(KLL) signals were recorded. Carbon Auger electrons were omitted in the analysis, since they overlap strongly with Auger electrons from the Ag substrate.

3. Results and discussion

Fig. 2 shows the results for a 10 ML thick film incoherent with the substrate. The maximum of the XPS yield of both C(ls) and O(ls) is clearly higher than the maximum of the oxygen Auger yield of $Y_{\mathrm{max}}^{\mathrm{O\text{-}Auger}} = 1.66 \pm 0.10$ (with the off-Bragg peak background normalized to unity), demonstrating differences in the underlying processes and the theoretical description.

In fact, the Auger yield can be described properly by Eq. (2) (with $F_{\mathrm{C}}^h = 0$), since the emission of Auger electrons is a secondary process, in which angular asymmetries are averaged out. The impact of indirect excitations due to electrons from the substrate is negligible under the present experimental conditions.

In contrast, the XPS yield generally has to be described by Eq. (3) [5,8]. Using Eq. (7) for the

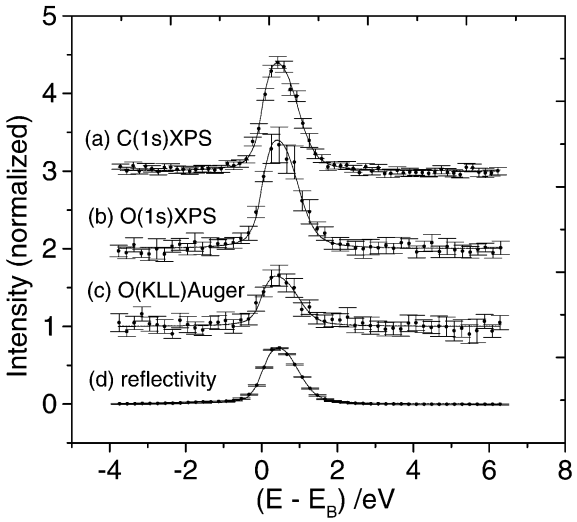

Fig. 2. XSW scans from a thick PTCDA film, which is incoherent with the substrate, i.e., whose coherent fraction, F_C^{111}, is about zero: (a) detection by C(ls) XPS; (b) detection by O(ls) XPS; (c) detection by O(KLL) Auger electrons; (d) Ag(1 1 1) reflectivity curve. The difference between detection by XPS (primary process) and Auger electrons (secondary process) is used for the analysis of non-dipolar contributions. Note that (a) and (b) are displaced relative to (c) for clarity. The solid lines are fits based on dynamical theory of diffraction.

case of $F_C^h = 0$, we can easily calculate the non-dipole parameter Q' from

$$Q' = \frac{[Y_{max} - 1] - R_{max}}{[Y_{max} - 1] + R_{max}}. \quad (8)$$

From the fits to the data shown in Fig. 2 we obtain for both C(1s) and O(1s) the parameters $Q' = 0.31 \pm 0.03$ and $\gamma' = Q'/\cos\theta_p = 0.44 \pm 0.04$.

According to calculations of multipole corrections for isolated atoms [11] at electron energies of 2 keV we should expect $\gamma'_{th} = 0.331$ for C ($Z = 6$). For Ne ($Z = 10$) these calculations [11] for the same photoelectron energies give $\gamma'_{th} = 0.306$. So, for oxygen ($Z = 8$) γ'_{th} is expected to be between 0.31 and 0.33. Calculations with results in the same range can be found in Refs. [12,13].

The reason for this discrepancy between γ'_{th} and γ'_{exp} is presently not understood. One issue is the possible difference between an isolated atom bound in a molecule or solid. While the effect on the ls states should be small, it may still have a detectable impact, since bonding changes the spherical symmetry. This would be an important observation, since then such measurements would provide a very sensitive test for the changes of the photoelectron interaction or potential in the atom due to bonding and, as a result, for the radial wave functions and partial wave shifts. However, more experiments on different materials are required to clarify this point.

Recently, similar non-dipole effects were investigated experimentally for incoherent films containing oxygen and fluorine on Cu(1 1 1) and Ni(1 1 1) substrates [7]. While the raw experimental data in terms of the difference between Auger and XPS detection appear to be consistent with those presented here (suggesting also similar Q' values), Q' values inconsistent with the present ones were reported.

Finally, we comment on the consequences of non-dipole effects for the analysis of XSW data from (coherent) monolayers ($F_C^h > 0$). Setting the detector angle close to the direction perpendicular to the incoming X-ray beam ($\theta_p \simeq 90°$) minimizes quadrupole contributions, but technically this is not possible for all chamber geometries. Therefore, generally, for XPS detection, Eq. (3) should be used rather than Eq. (2), but this requires the determination of the non-dipolar corrections. While the most significant correction, γ', can be obtained from a comparison with a thick incoherent film (which also affords a high signal) as shown in the present work, γ'' can only be accessed for $F_C^h > 0$. One way to access γ'' would be to record simultaneously both the XPS and the Auger yield for a (coherent) monolayer (to be analyzed by Eqs. (3) and (2), respectively), but for light elements the signal may be very weak. Moreover, for Auger detection in coherent monolayers, secondary excitation from the substrate can have an impact on the signal [14]. Another way to address the non-dipolar issues is the use of higher-order Bragg reflections (e.g., (2 2 2)), since this adds an independent data point, but it may require additional experimental efforts due to the correspondingly higher photoelectron energies. We note that from theory [11], we expect γ'' to be of the order of 0.08

for conditions employed in the present experiment. Future experiments will be devoted to addressing γ''.

In conclusion, we have determined the strongest non-dipolar contribution, γ', in XPS yields from XSW. The knowledge of non-dipolar parameters is crucial for a proper analysis of XSW data with XPS detection. In addition, the unique properties of XSWs with the defined spatial phase of the exciting wave allow the determination of both the amplitude and the phase from quadrupole contributions in photoelectric scattering, which are difficult to access with other methods.

Acknowledgements

The authors wish to acknowledge financial support from the Max-Planck-Gesellschaft. They benefited from interactions with J. Pflaum, B. Krause, A.C. Dürr, V. Kruppa, and N. Karl.

References

[1] J. Zegenhagen, Surf. Sci. Rep. 18 (1993) 199.
[2] D.E. Woodruff, Prog. Surf. Sci. 57 (1998) 1.
[3] L.E. Berman, M.J. Bedzyk, Phys. Rev. Lett. 63 (1989) 1172.
[4] I.A. Vartanyants, J. Zegenhagen, Il Nuovo Cimento D 19 (1997) 617.
[5] I.A. Vartanyants, J. Zegenhagen, Phys. Stat. Sol. (b) 215 (1999) 819.
[6] C.J. Fisher, R. Ithin, R.G. Jones, G.J. Jackson, D.P. Woodruff, B.C.C. Cowie, J. Phys.: Condens. Matter 10 (1998) L623.
[7] G.J. Jackson, B.C.C. Cowie, D.P. Woodruff, R.G. Jones, M.S. Kariapper, C. Fisher, A.S.Y. Chan, M. Butterfield, Phys. Rev. Lett. 84 (2000) 2346.
[8] I.A. Vartanyants, J. Zegenhagen, Solid State Commun. 113 (1999) 299.
[9] S.R. Forrest, Chem. Rev. 97 (1997) 1793.
[10] P. Fenter, F. Schreiber, L. Zhou, P. Eisenberger, S.R. Forrest, Phys. Rev. B 56 (1997) 3046.
[11] A. Bechler, R.H. Pratt, Phys. Rev. A 39 (1989) 1774.
[12] J. Cooper, Phys. Rev. B 47 (1993) 1841.
[13] V.I. Nefedov, V.G. Yarzhemskii, I.S. Nefedova, M.B. Trzhaskovskaya, I.M. Band, Doklady Phys. 44 (1999) 423.
[14] A.G. Shard, B.C.C. Cowie, J. Phys.: Condens. Matter 10 (1998) L69.